VNU Journal of Science: Mathematics - Physics

Journal homepage: https://js.vnu.edu.vn/MaP

Original Article

Structure and Magnetic Properties of $SrFe_{12}O_{19}/CoFe_2O_4$ Nanocomposite Ferrite

Tran Thi Viet Nga[1,*], Nguyen Thi Lan[2], To Thanh Loan[1], Hoang Ha[1]

[1]*International Training Institute for Materials Science (ITIMS) Hanoi University of Technology, 01 Dai Co Viet, Hanoi, Vietnam*

[2]*Advanced Institute for Science and Technology (AIST) Hanoi University of Technology, 01 Dai Co Viet, Hanoi, Vietnam*

Received 25 January 2019
Revised 23 May 2019; Accepted 28 May 2019

Abstract: Nanocomposite particles $SrFe_{12}O_{19}/ CoFe_2O_4$ were synthesized by sol-gel method. The nanocomposites are formed at the calcining temperature around 850 ºC in 5 hours. The phase composition, surface morphology and magnetic properties of the nanocomposites were investigated using XRD, SEM and VSM, respectively. The results show that the magnetic properties of nanocomposite particles are strongly influenced by the molar ratios of the hard and soft phases and particle size distributions. The samples with the mass ratio of R_m= $SrFe_{12}O_{19}/ NiFe_2O_4$ = 1/3 and 1/5 are characterized with a "bee waist" type hysteresis loop. While all the samples R_V show an excellent smooth hysteresis loop and a single – phase magnetization behavior. The coercivity decreases significantly and the magnetization drastically increases with decreasing of volume ratio R_V.

Keywords: nanocomposite, sol- gel method, exchange coupling.

1. Introduction

Nanocomposite magnetic materials consisting of soft and hard magnetic phases have become a hot research topic in recent time because of potential applications in the fields of science and technology. For example, magnetic micro electromechanical systems (MEMS) including microactuators, sensors, recording heads and micro-motors, spins of electron devices apply in spin- valve read heads [1-4]. Theoretically, by combining high magnetic anisotropy of magnetically hard phase and the high saturation magnetization of magnetically soft phase can enhance their magnetic properties. However,

*Corresponding author.
Email address: vietnga@itims.edu.vn

https//doi.org/ 10.25073/2588-1124/vnumap.4319

the magnetic properties of nanocomposite materials depend strongly on the grain size, structure and morphology of phases, distribution of the magnetically hard and soft phases, and impurity. Numerous efforts have recently been made into the fabrication of nanocomposite particles to enhance exchange coupling interaction by controlling the particle size and distribution particles. A mong the hard materials (NdFeB, $SmCo_5$, FePt…), strontium ferrite (SrM) has high coercivity H_C, large magneto- crystalline anisotropy [5] and excellent chemical stability [6]. It is well known that $CoFe_2O_4$ is a spinel ferrite, which possesses higher saturation, remanent magnetization and coercivity compared with other spinel ferrites ($NiFe_2O_4$, $MnFe_2O_4$, …) [7]. Therefore, in the exchange spring magnet, mixing of SrM- hard phase and $CoFe_2O_4$ phase could utilize the superior magnetic properties of two phases. The recent research work showed that the ferrite particles can be obtained via the chemical methods such as co-precipitation, hydrothermal [8, 9], sol–gel [10, 11]. Moreover, the ferrites can be successfully synthesized at a relatively low temperature without subsequent sintering at high temperature. That may be beneficial to control the growth of crystallites. So, we only need a relatively lower sintering temperature to achieve the homogeneous ferrite particles and a strong exchange coupling. In this work, $SrFe_{12}O_{19}/CoFe_2O_4$ nanocomposite have been prepared by sol- gel method.

2. Experiment

Synthesis of $SrFe_{12}O_{19}$ and $CoFe_2O_4$ powders

$SrFe_{12}O_{19}$ and $CoFe_2O_4$ nanopowders were synthesized separately by via sol-gel method. $Fe(NO_3)_3 \cdot 9H_2O$, $Sr(NO_3)_2$ and $Co(NO_3)_2 \cdot 6H_2O$ were dissolved in deionized water to form an aqueous solution of 1M. The nitrates used to synthesize $SrFe_{12}O_{19}$ and $CoFe_2O_4$ were dissolved in deionized water with the molar ratio Sr/Fe is 11.5 and Co/Fe is 2. Citric acid (AC) was then added into the solution at fixed $[Sr^{2+} + Fe^{3+}]$:AC and $[Co^{2+} + Fe^{3+}]$: AC molar ratio of 1:3. NH_4OH was used to adjust the pH to 1. After the pH had been stabilized, the solution was stirred at 1000 rpm and gradually evaporated at 90 °C. As the water evaporated, the remainder became highly viscous gels as a result of the chelation process. These gels were dried at 90 °C for 24 h, and then heated at 450 °C (for $SrFe_{12}O_{19}$) and 200 °C (for $CoFe_2O_4$) for 2 hours to eliminate the remaining residual water and other organic impurities (aerogels were formed). To form the hexaferrite and spinel phase, the gels were calcined in air at 850°C for 5 hours.

Preparation of $SrFe_{12}O_{19}$ /$CoFe_2O_4$ nanocomposites

The first series of specimens $SrFe_{12}O_{19}/CoFe_2O_4$ nanopowders were synthesized using the aerogel powders obtained previously. $SrFe_{12}O_{19}$ and $CoFe_2O_4$ aerogel powders were uniformly mixed with mass ratios (R_m) of 1:1, 1:3, 1:5 and 1:7, denoted as R_m11, R_m13, R_m15 and R_m17, respectively. Then the mixtures were pressed into platelets of 6 mm in diameter and sintered at 850 °C for 5 hours.

The second series of specimens, the $SrFe_{12}O_{19}/CoFe_2O_4$ nanocomposite powders were synthesized by one step sol-gel method. Stoichiometric amounts of $Fe(NO_3)_3 \cdot 9H_2O$, $Sr(NO_3)_2$, $Co(NO_3)_2$ were dissolved completely in deionized water. In these processes, the ratio of Sr^{2+}/Fe^{3+} and Fe^{3+}/Co^{2+} were fixed at 11.5 and 2. The ratio R_V of (Sr^{2+}/Fe^{3+}) : (Fe^{3+}/Co^{2+}) was fixed at 1:1, 1:3, 1:5 and 1:7. Citric acid was then added into the solution at a fixed $(Sr^{2+} + Fe^{3+} + Co^{2+})$/AC volume ratio of 1/3. NH_4OH in aqueous form was added to the mixed solutions and the pH of the solutions was adjusted to about 1. The mixtures were stirred at 1000 rpm and slowly evaporated at 90 °C to form gels. These gels were dried at 90 °C for 24 h and then heated at 350 °C for 2 hours to eliminate the remaining residual water and other organic impurities. An equal weight of the produced ferrite powders was compressed into

briquettes of 6 mm diameters and 3 g weight. The composites were annealed in air at 850 ºC for 5 h. The samples were marked as R_V11, R_V13, R_V15 and R_V17.

Characterization

The crystal structure and phases of the obtained samples were identified via X-ray powder diffraction (XRD) using a Siemens D5000 diffractometer (CuKα radiation, λ = 1.54056 Å). Morphological features and particle size were observed by scanning electron microscopy (SEM, JEOL-JSM 7600F). The magnetic were measured using a vibrating sample magnetometer (VSM, Lakeshore 7410) with applied magnetic fields up to 10 kOe. Thermogravimetric analyses (TGA) were employed to study thermal behavior using a Universal V2960T with a heating rate of 10 °C/min in air, whereas pure alumina powder was used as the reference specimen.

3. Result and discussions

The TGA of gel precursor with $R_V = 1$ are shown in the Fig. 1. The experiment was performed using 23.224 mg of gel precursor and a heating of 10 ºC/ min in static air. The first exothermic peak at approximately 152 ºC was attributed to the decomposition of NH_4NO_3 to liberate NO, O_2, and H_2O and the weight loss of 45%. The second exothermic peak at approximately 230 ºC showed the decomposition of the remaining unreactive organic material induced by excess citric and weight loss of 67.4% (Fig. 1 a). At the approximately 549 ºC and 730 ºC, the weight loss about 70.55% (Fig. 1 b). At higher temperature, the weight has not decreased. Based on the results obtained from the thermal analysis of the composite precursor (Fig. 1), we choose the temperature of 350 ºC for heating gels and eliminating the remaining residual water and other organic impurities.

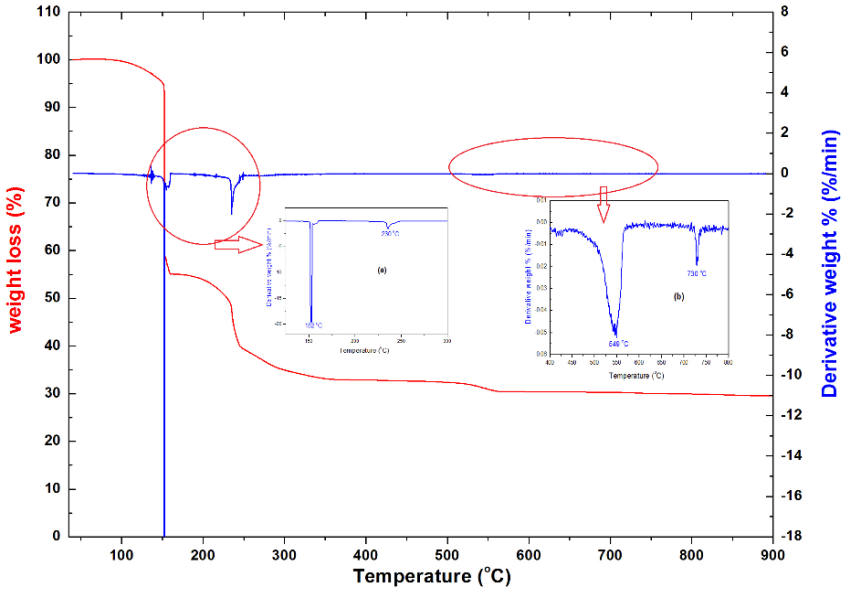

Figure 1. Thermogravimetric (TGA) curve of the gel precursor at $R_V = 1$.

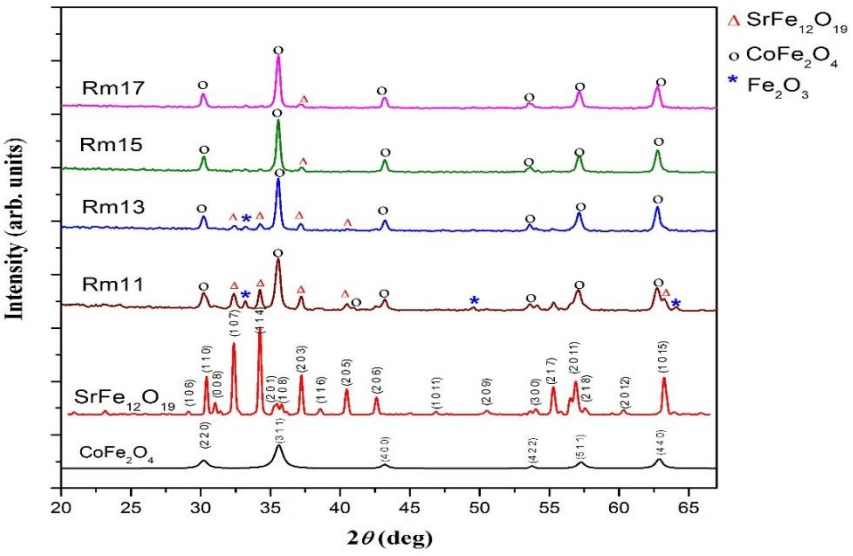

(a)

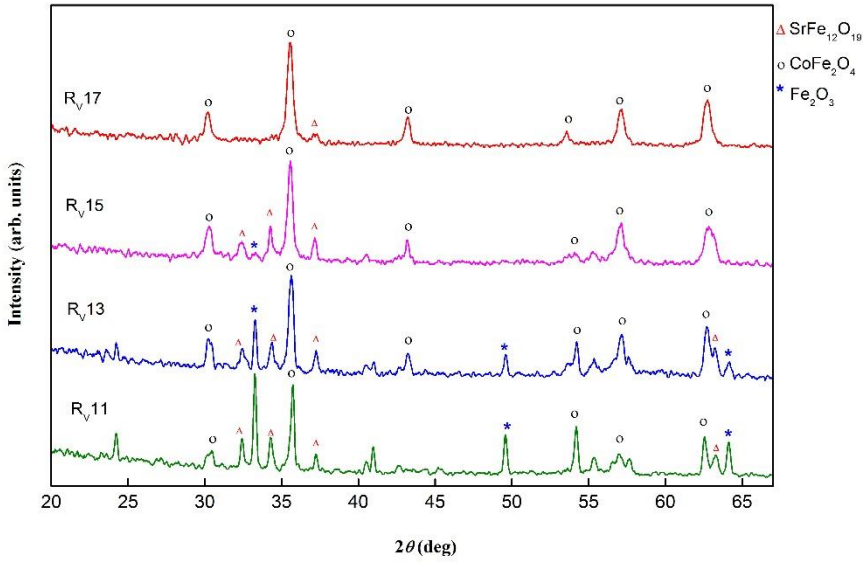

(b)

Figure 2. XRD patterns of the $SrFe_{12}O_{19}/CoFe_2O_4$ nanocomposite powders calcination at 850 ^oC for 5 hours (a) R_m and (b) R_V.

The XRD patterns of the $SrFe_{12}O_{19}$, $CoFe_2O_4$ and $SrFe_{12}O_{19}/CoFe_2O_4$ nanocomposites powders with various of R_m and R_V are shown in the Fig.2. It can be clearly seen that the $SrFe_{12}O_{19}$ and $CoFe_2O_4$ samples are single phase after calcination at 850 ^oC for 5 hours. While all nanocomposite samples composed of $SrFe_{12}O_{19}$, $CoFe_2O_4$ phases and a small amount of impurity phase of α- Fe_2O_3. This observation was also reported by other authors and may be attributed to the occurrence of local combustion during calcination [12, 13]. XRD refinements were carried out using the Rietveld method

with the help of the Fullprof program. The percentages of phases present in these samples and lattice parameters (*a, c*) are listed in Table 1. The percentages of α- Fe_2O_3 impurity phase decreases with increasing of concentration $CoFe_2O_4$ at all nanocomposite samples. According to Wei Zhong et al. [14], the preliminary heating process at temperatures between 300 °C and 500 °C could further enhance the development of Sr-ferrite after calcination and remove α- Fe_2O_3 impurity phase. For R_m samples, the aerogels of $SrFe_{12}O_{19}$ and $CoFe_2O_4$ were heated at 450 ºC and 200 ºC before mixing. And for R_V samples, the aerogels of nanocomposite samples were heated at 350 ºC. Therefore, the percentage of α- Fe_2O_3 impurity phase in R_m samples are smaller than that of α- Fe_2O_3 impurity phase in R_V samples. It can be concluded that using the sol – gel method to prepare nanocomposite samples need higher preliminary heating temperature (>350 ºC).

Table 1. Lattice parameters (a, c) and percentages of phases present in the obtained samples

Sample	Phase	*a* (Å)	*c* (Å)	%
$SrFe_{12}O_{19}$	$SrFe_{12}O_{19}$	5,8723	23,0247	
$CoFe_2O_4$	$CoFe_2O_4$	8,398		
	$SrFe_{12}O_{19}$	5,873	23,024	42,58
R_m11	$CoFe_2O_4$	8,312		48,59
	α -Fe_2O_3			8,83
	$SrFe_{12}O_{19}$	5,8752	23,018	21,76
R_m13	$CoFe_2O_4$	8,326		71,21
	α -Fe_2O_3			7,03
	$SrFe_{12}O_{19}$	5,8754	23,023	8,80
R_m15	$CoFe_2O_4$	8,3305		83,65
	α -Fe_2O_3			7,55
	$SrFe_{12}O_{19}$	5,8736	23,017	2,90
R_m17	$CoFe_2O_4$	8,3218		91,13
	α -Fe_2O_3			5,97
	$SrFe_{12}O_{19}$	5,8765	23,027	36,29
R_v11	$CoFe_2O_4$	8,3313		11,32
	α -Fe_2O_3			52,39
	$SrFe_{12}O_{19}$	5,8781	23,03	34,63
R_v13	$CoFe_2O_4$	8,3135		39,30
	α -Fe_2O_3			26,7
	$SrFe_{12}O_{19}$	5,873	23,027	38,24
R_v15	$CoFe_2O_4$	8,326		47,47
	α -Fe_2O_3			14,03
	$SrFe_{12}O_{19}$	5,8756	23,0168	7,41
R_v17	$CoFe_2O_4$	8,323		92,59
	α -Fe_2O_3			0

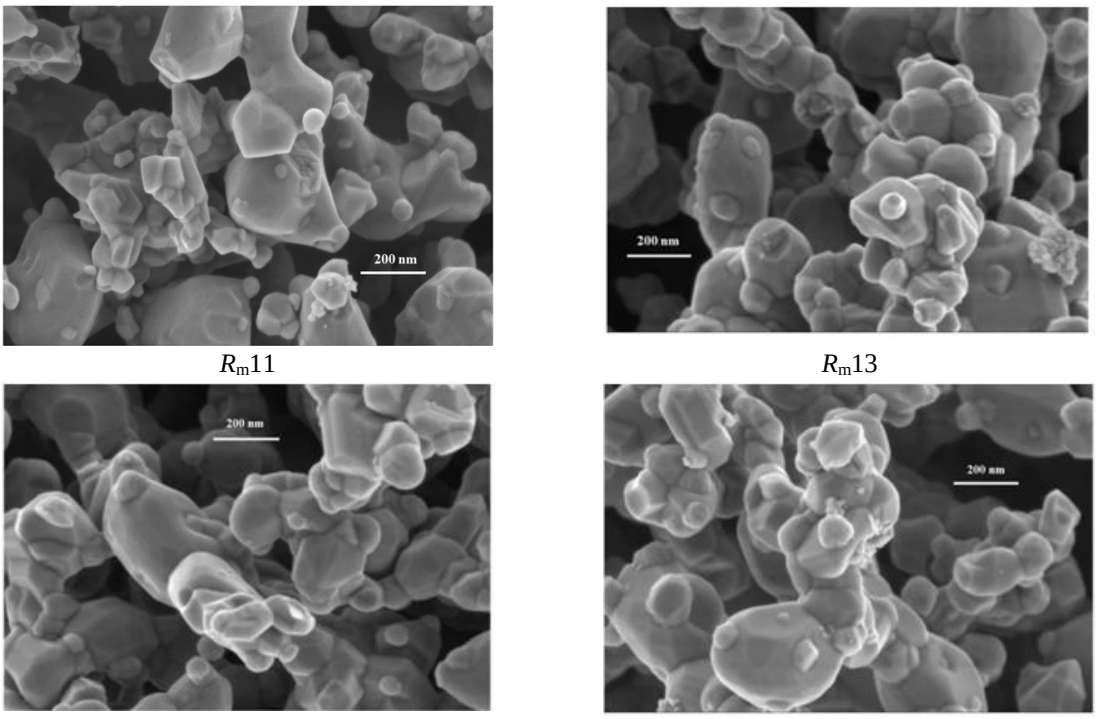

R_m11 R_m13

R_m15 R_m17

Figure 3. SEM images of the $SrFe_{12}O_{19}/CoFe_2O_4$ nanocomposite samples with different mass ratios (R_m) calcinated at 850 °C for 5 h.

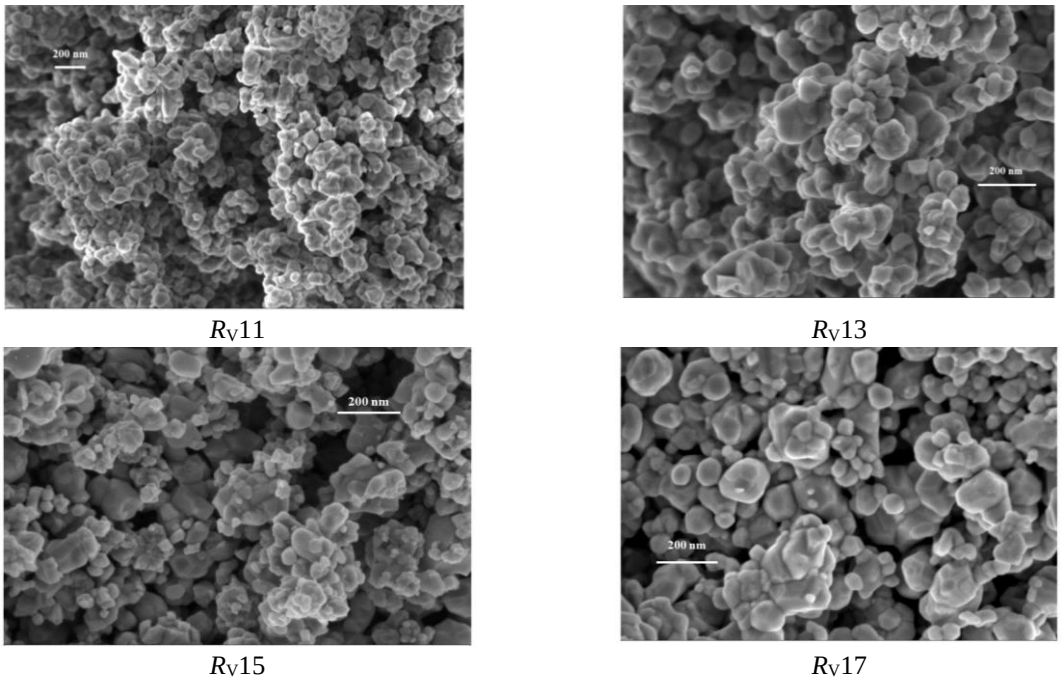

R_V11 R_V13

R_V15 R_V17

Figure 4. SEM images of the $SrFe_{12}O_{19}/CoFe_2O_4$ nanocomposite samples with different volume ratios (R_V) calcinated at 850 °C for 5 h.

The SEM images of $SrFe_{12}O_{19}/CoFe_2O_4$ nanocomposites with different mass and volume ratios of phases are illustrated in Fig. 3 and 4. Fig. 3 shows SEM micrographs of Rm samples. We can see that cubic grains with smaller size are distributed in a matrix of hexagonal grains with lager size. The hexagonal plate- like and cubic grains have approximate diameter from 50 nm to 100 nm and 30 nm to 50 nm, respectively. Fig. 4 shows SEM micrographs of R_V composite samples. As can be seen from figure, two phases are well distributed, and the grain size is about 50 – 100 nm.

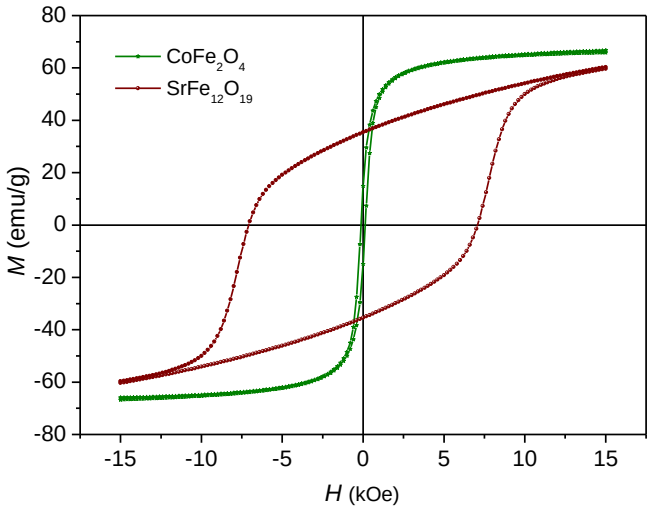

Figure 5. Hysteresis loops of the $SrFe_{12}O_{19}$ and $CoFe_2O_4$ samples annealed at 850 ^oC for 5 h.

Figure 5 depicts the hysteresis loops at room temperature of $SrFe_{12}O_{19}$ and $CoFe_2O_4$ nanoparticles. The $SrFe_{12}O_{19}$ nanoparticles exhibit a magnetically hard behavior with the coercivity of 7 kOe and saturation magnetization of 60 emu/g. The hysteresis loop of $CoFe_2O_4$ nanoparticles shows a magnetically soft behavior with the intrinsic coercivity of 0.314 kOe and saturation magnetization of 66 emu/g. It has been reported that the theoretical value of saturation magnetization for $SrFe_{12}O_{19}$ and $CoFe_2O_4$ is 74 emu/g and 91 emu/g, respectively. As seen in the Fig. 6a, the samples R_m11 and R_m17 exhibit a smooth hysteresis loop and show a single-phase magnetization behavior, although their crystallo- graphically compose of two phases. While R_m13 and R_m15, the hysteresis loop exhibits a typical "bee waist". These results were in agreement with those reported by Moon K. W et. al [15]. In this study, the BaM+ x%$NiZnFe_2O_4$ nanocomposite particles were fabricated by a self- propagating combustion method. As can be seen, the coercivity H_C decrease with decreasing concentration of $SrFe_{12}O_{19}$. It may be due to the fact the H_C of $CoFe_2O_4$ is smaller than that of $SrFe_{12}O_{19}$. The magnetization M of R_m11 and R_m13 are comparatively lager as compared with that of $SrFe_{12}O_{19}$ sample, owing to the present of $CoFe_2O_4$ phase. However, for R_m15 and R_m17, the value of magnetization M reduce tendency. The non- homogeneous distribution of phases can be a reason for the change of magnetization M. Thus, physical mixing method is an inadequate method for obtaining exchange- spring magnets because of non- homogenous distribution of magnetic phases (Fig. 3).

All the samples R_V show an excellent smooth hysteresis loop and a single – phase magnetization behavior. It indicates the hard and soft magnetic phases are switching individually due to the incomplete exchange- coupling [16-17]. The magnetization at 10 T (M), remanence magnetization (M_r) and coercivity (H_C) obtained from hysteresis loops are showed in Table 2.

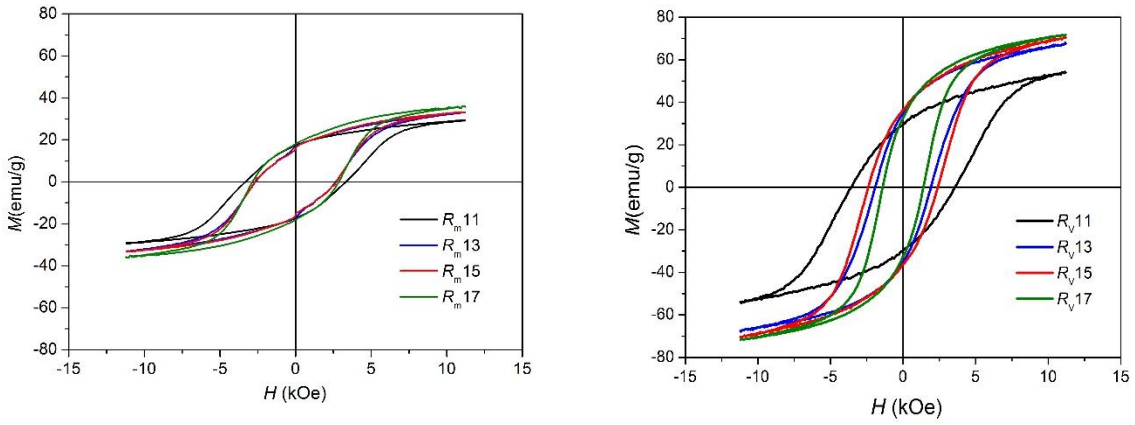

(a) (b)

Figure 6. Hysteresis loops of the $SrFe_{12}O_{19}/CoFe_2O_4$ nanocomposite samples (a) R_m and (b) R_V calcination at 850 ^oC for 5 hours.

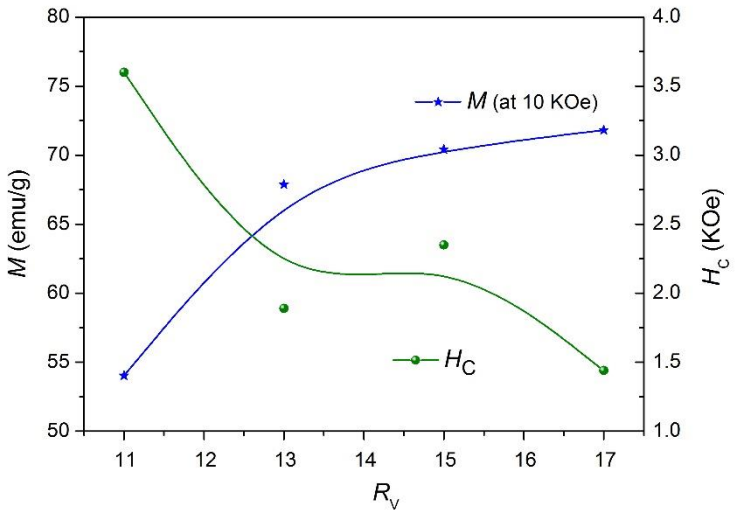

Figure 7. The variation in magnetization M (at 10 kOe) and coercive force (H_C) with decreasing of the volume ratio R_V.

The dependence of magnetization M (at 10 kOe) and coercivity H_C on ratio R_V is shown in Fig. 7. As expected, the magnetic properties of nanocomposite particles can be enhanced with a strong exchange coupling. However, we can see that the coercive force decreases with increasing concentration of soft magnetically phase $CoFe_2O_4$. As concentration of the soft phase increases, the role of dipolar interactions among the soft grains becomes more important [18] and the reverse domains in soft phase with low nucleation field nucleate readily. Thus, the value of H_C decreases. In addition, the presence of α-Fe_2O_3 phase could be a reason for the decreasing of coercivity. This result has been found in the $SrFe_{12}O_{19}/CoFe_2O_4$ [17], $BaFe_{12}O_{19}/Fe_3O_4$ [19] and $BaFe_{12}O_{19}/Ni_{0.5}Zn_{0.5}Fe_2O_4$ [20]. The value of coercivity H_C markedly decreases from 3.6 kOe to 1.44 kOe while the magnetization M increases from 54.02 emu/g to 71.81 emu/g when the ratio R_V decreases from 1:1 to 1:7 (table 2). The magnetization M

of R_V17 is larger about 8% and 19.6% than that of $CoFe_2O_4$ and $SrFe_{12}O_{19}$, respectively. Compare with R_m samples, the magnetization M of R_V samples is higher than that of R_m samples. The enhancement of magnetization can be assigned to the homogeneously distributed phases and the improving of exchange interaction between the hard and soft grains.

Table 2. Magnetization at 10 kOe (M), coercive force (H_C) and remanence magnetization (M_r) at room temperature of the $SrFe_{12}O_{19}/NiFe_2O_4$ nanocomposite powders with different ratios R_m, R_V.

Sample	H_C (kOe)	M at 10 kOe (emu/g)	M_r (emu/g)
Rm11	3.32	64	35.92
Rm13	2.69	62.89	32.28
Rm15	2.69	33.18	16.62
Rm17	2.92	36.05	18.19
R_V11	3.6	54.02	28.92
R_V13	1.89	67.87	34.21
R_V15	2.35	70.42	35.91
R_V17	1.44	71.81	33.17

4. Conclusions

In summary, the $SrFe_{12}O_{19}/CoFe_2O_4$ nanocomposites with exchange coupling behavior have been prepared successfully by sol gel method. XRD patterns confirmed the coexistence of two hard and soft phases together with a small amount of impurity phase of α- Fe_2O_3. Nanocomposites prepared by physical mixing method, showed a typical "bee waist" type hysteresis loop and non- homogenous formation of two phases. The SEM micrographs of nanocomposites R_V showed homogenous formation of two phases and particle size distribution is about 50 – 100 nm. The hysteresis loop of the samples R_V behaves like a single magnetic phase, indicating a strong exchange coupling between two magnetically phases. The coercivity H_c decreases from 3.6 kOe to 1.44 kOe and the magnetization M increases from 54 to 71.81 emu/g with decreasing of ratio volume R_V from 1/1 to 1/7.

Acknowledgments

This research was funded by the Vietnam National Foundation for Science and Technology Development under grant number 103.02-2017.16

References

[1] D.A. Allwood, G. Xiong, M.D. Cooke, C.C. Faulkner, D. Atkinson, N. Vernier, R.P. Cowburn, Submicrometer Ferromagnetic NOT Gate and Shift Register, Science. 296 (2002) 2003–2006.

[2] F.X. Redl, K.S. Cho, C.B. Murray, S. O'Brien, Three-dimensional binary superlattices of magnetic nanocrystals and semiconductor quantum dots, Nature. 423 (2003) 968–971.

[3] Z.L. Wang, X.J. Liu, M.F. Lv, P. Chai, Y. Liu, X.F. Zhou, J. Meng, Preparation of One-Dimensional CoFe2O4 Nanostructures and Their Magnetic Properties, J. Phys. Chem. C. 112 (2008) 15171–15175.

[4] S.O. Hwang, C.H. Kim, Y. Myung, S. Park, J. Park, J. Kim, C. Han, Synthesis of Vertically Aligned Manganese-Doped Fe_3O_4 Nanowire Arrays and Their Excellent Room-Temperature Gas Sensing Ability, J. Phys. Chem. C. 112 (2008) 13911–13916.

[5] M. A. Moskalenko, V.M. Uzdin, H. Zabel, Manipulation by exchange coupling in layered magnetic structures, J. Appl. Phys. 115 (2014) 053913.

[6] Gu FM, Pan WW, Liu QF, Wang JB. Electrospun magnetic $SrFe_{12}O_{19}$ nanofibres with improved hard magnetism, J. Phys. D-Appl. Phys. 46 (2013) 445003– 10.

[7] Rakshit R, Mandal M, Pal M, Mandal K. Tuning of magnetic properties of $CoFe_2O_4$ nanoparticles through charge transfer effect , Appl. Phys. Lett. 104 (2014) 092412– 0912417.

[8] A.L. Xia, C.H. Zuo, L. Chen, C.G. Jin, Y.H. Lv, Hexagonal $SrFe_{12}O_{19}$ ferrites: Hydrothermal synthesis and their sintering properties, J. Magn. Magn. Mater. 332 (2013) 186-191.

[9] A.L. Xia, X.Z. Hu, D.K. Li, L. Chen, C.G. Jin, C.H. Zuo, S.B. Su, Facile hydrothermal synthesis of core/shell-like composite $SrFe_{12}O_{19}$/(Ni,Zn)Fe_2O_4 nanopowders and their magnetic properties, Electron. Mater. Lett. 10 (2014) 423-426.

[10] B.N. Pianciola, E. Lima Jr., H.E. Troiani, L.C.C.M. Nagamine, R. Cohen, R.D. Zysler, Size and surface effects in the magnetic order of $CoFe_2O_4$ nanoparticles , J. Magn. Magn. Mater. 377 (2015) 44-51.

[11] C.N. Chinnasamy, B. Jeyadevan, K. Shinoda, K. Tohji, D.J. Djayaprawira, M. Takahashi, R.J. Joseyphus, A. Narayanasamy, Unusually high coercivity and critical single-domain size of nearly monodispersed $CoFe_2O_4$ nanoparticles, Appl. Phys. Lett. 83 (2003) 2862-2864.

[12] Haibo Yang, Miao Liu, Ying Lin, Guoqiang Dong, Lingyan Hu, Ying Zhang, Jingyi Tan, Enhanced remanenc e and (BH) max of $BaFe_{12}O_{19}$ /$CoFe_2O_4$ composite ceramics prepared by the microwave sintering method, Materials Chemistry and Physics. 160 (2015) 5-10.

[13] Juan Dong, Yi Zhang, Xinlei Zhang, Qingfang Liu, Jianbo Wang, Improved magnetic properties of $SrFe_{12}O_{19}$/FeCo core–shell nanofibers by hard/soft magnetic exchange–coupling effect, Materials Letters. 120 (2014) 9-12.

[14] Wei Zhong, Weiping Ding, Ning Zhang, Jianming Hong, Qijie Yan, Youwei Du , Key step in synthesis of ultrafine $BaFe_{12}O_{19}$ by sol-gel technique, J. Magn. Magn. Mater. 168 (1997) 196-202.

[15] K. W. Moon, S. G. Cho, Y. H. Choa, K. H. Kim, and J. Kim, Synthesis and magnetic properties of nano Ba-hexaferrite/NiZn ferrite composites, phys. stat. sol. (a) 204 (12) (2007) 4141 – 4144.

[16] Y.H. Liu, S.G.E.T. Velthuis, J.S. Jiang, Y. Choi, S.D. Bader, A.A. Parizzi, H. Ambaye, V. Lauter, Magnetic structure in Fe/Sm-Co exchange spring bilayers with intermixed interfaces, Phys. Rev. B. 83 (2011) 174418.

[17] Ailin Xia, Suzhen Ren, Junshu Lin, Yue Ma, Chen Xu, Jinlin Li, Chuangui Jin, Xianguo Liu, Magnetic properties of sintered $SrFe_{12}O_{19}$-$CoFe_2O_4$ nanocomposites with exchange coupling, J. Alloys Compd. 653 (2015) 108- 116.

[18] C.B. Rong, H.W. Zhang, R.J. Chen, S.L. He, B.G. Shen, The role of dipolar interaction in nanocomposite permanent magnets, J. Magn. Magn. Mater. 302 (2006) 126.

[19] K.P. Remya, D. Prabhu, S. Amirthapandian, C. Viswanathan, N. Ponpandian, Exchange spring magnetic behavior in $BaFe_{12}O_{19}$ /Fe_3O_4 Nanocomposites, J. Magn. Magn. Mater. 406 (2016) 233 – 238.

[20] Rui Xiong, Weiwei Li, Chunlong Fei, Yong Liu, Jing Shi, Exchange-spring behavior in $BaFe_{12}O_{19}$ -$Ni_{0.5}Zn_{0.5}Fe_2O_4$ nanocomposites synthesized by a combustion method, Ceramics International. 42 (2016) 11913-11917.